

Supporting Information

Biomimetic closed-loop recyclable, long-term durable, extreme-condition resist, fire-fighting protective nanocoating enabled by reversible flocculation assembly

Jiayan Zhang, Furong Zeng, Bowen Liu, Zihao Wang, Xincen Lin, Haibo Zhao*, Yuzhong Wang*

The Collaborative Innovation Center for Eco-Friendly and Fire-safety Polymeric Materials, National Engineering Laboratory of Eco-Friendly Polymeric Materials (Sichuan), State Key Laboratory of Polymer Materials Engineering, College of Chemistry, Sichuan University, Sichuan 610064 (China)

*Corresponding author. E-mail: haibor7@163.com, polymers@vip.126.com

Table of Contents

Materials	3
Preparation of PAM/SEP Complexes	3
Preparation of PAM/SEP coated foam	3
Density Functional Theory (DFT) Calculations	4
Cycle Process of Flocculation Assembly-disassembly-recovery Experiment	4
Durability Tests	6
General Characterization.....	6
Figure S1-S26.....	8
Table S1-S6.....	34

Materials

Anionic polyacrylamide (HPAM, $M_w = 100000$) was purchased from Sigma-Aldrich. Sepiolite (SEP) was purchased from Hebei Zongrun Mineral Products Co., Ltd. Concentrated hydrochloric acid (HCl, 36.5%) and sodium hydroxide (NaOH) were supplied by Kelong Chemical Reagent Company (Chengdu, China). Flexible polyurethane foam (PU, DW30) was purchased from Shenzhen Hongchengxing Sponge Material Co., Ltd. Deionized water (DI water) with a resistance of 18 M Ω cm was used in all experiments.

Preparation of PAM/SEP Complexes

The PAM/SEP complexes were prepared by hydrogen bonding interactions in neutral aqueous solution. 0.5 g PAM was fully dissolved in 100 mL DI water aqueous solution (0.5 wt%, pH= 7). The sepiolite suspension (1.0 wt%, pH = 7) was dispersed and stabilized by sonication for 1 h. Then, the above two substances were uniformly mixed together with a 1:1 volume ratio, obtaining a continuously distributed PAM/SEP aggregation network. The pH of the mixed PAM/SEP system was controlled in the range of 4-10 by dripping 1 M HCl or NaOH, and then the system was shaken to make it fully mixed and stabilized for 2 hours to observe the changes.

Preparation of PAM/SEP coated foam

The PAM/SEP-coated foam was fabricated in two steps. First, the pure foam (washed with ethanol and dried before treatment) was dipped in above PAM solution to form a network-like staggered coverage on the surface. Next, the PAM-coated foam was immersed in a certain amount of sepiolite suspension (maintained

30% weight gain for coated foam) to fix the sepiolite by flocculation assembly on the surface of the foam, and then remove the excess solution and the coating components without stable adhesion by squeezing process to obtain the stably adhered PAM/SEP coating on the foam. The weight gain (WG) was calculated by the following formula: $WG (\%) = (w_1 - w_0) / w_0 \times 100\%$, where w_0 represents the weight of the control foam and w_1 represents the weight of the coated foam.

Preparation of other inorganic particles coated foam

Other inorganic particles (GO, MMT, MWCNTs, ATH, MH, SiO₂) coated foams were prepared as follows. The inorganic particles suspension (1.0 wt%, pH = 7) was dispersed and stabilized by sonication for 1 h. The inorganic particles coated foam was fabricated in two steps. First, the pure foam (washed with ethanol and dried before treatment) was dipped in PAM solution to form a network-like staggered coverage on the surface. Next, the PAM-coated foam was immersed in a certain amount of inorganic particles suspension (maintained 30% weight gain for coated foam) to fix the inorganic particles by flocculation assembly on the surface of the foam and then, remove the excess solution and the coating components without stable adhesion by squeezing process to obtain the stably adhered PAM/SEP coating on the foam.. The weight gain (WG) was calculated by the following formula: $WG (\%) = (w_1 - w_0) / w_0 \times 100\%$, where w_0 represents the weight of the control foam and w_1 represents the weight of the coated foam.

Density Functional Theory (DFT) Calculations

Density functional theory calculations were carried out using Gaussian 16 programs throughout this manuscript. Geometric optimizations were performed with B3LYP-D3(BJ)/def-TZVP theoretical level. Harmonic vibration frequency calculations were performed for all stationary points to confirm them as a local minima (Nimag=0). Approximate solvent effects of water were taken into consideration based on the integral

equation formalism variant of polarizable continuum model (IEFPCM) in all DFT calculations. A tetrahedral surface model (containing a hexagon formed by six SiO₄ tetrahedra) of sepiolite was employed. The optimized structures were rendered by VMD program. The surface analysis of electrostatic potential (ESP) has been carried out using Multiwfn.

Accordingly, the interaction energy (E_{ads}) is calculated using the equation:

$$E_{ads} = E(\text{complex}) - E(a) - E(b)$$

where E_{ads} is the adsorption energy of PAM/SEP complex at different pH states.

Where E (complex), E (a) and E (b) are total energies of the complexes, PAM and Sepiolite, respectively.

Cycle Process of Flocculation Assembly-disassembly-recovery Experiment

To evaluate the disassembly of the coated foams under different pH conditions, the PAM/SEP coated foams were placed in aqueous solutions with a pH in the range of 4-14 for 2 h and then subjected to 30 manual squeeze-release cycles before drying. Then the coating components disassembled at pH=10 were filtered and the solid components were collected and dried, whereby the coating was recovered for further reassembly. Finally, the collected solid components and the supplemented sepiolite were dispersed in water to reach a target concentration, and then they were reused according to the method of initial assembly of the PAM/SEP coated foam. Then, the masses of the original foams (m_0), the coated samples (m_c), the disassembled samples (m_d), and the recycled coating components (m_r) were recorded. The disassembly efficiency (D (%)) and recycle efficiency (R (%)) were calculated by the following formulas:

$$D(\%) = \frac{m_c - m_d}{m_c - m_0} \times 100\%$$

$$R(\%) = \frac{m_r}{m_c - m_0} \times 100\%$$

Durability Tests

To assess the durability against water and organic solvents, the coated foams were soaked in water and various organic solvents (methanol, acetone, ether, toluene, and hexane) for several days. After that, the foams were extracted and dried at 80 °C for 4 h for further study. The hydrothermal aging test was carried out by placing the sample in a high and low temperature damp heat aging box (105 °C · 100% RH) for 3 h, according to GB/T 9640-2008 standard.

General Characterization

The morphologies of samples were studied by scanning electron microscopy (SEM, JSM-7500F JEOL) at an accelerating voltage of 15 kV. Fourier transform infrared (FT-IR) spectra were obtained on a Nicolet 6700 instrument (Thermo Fisher Scientific Co., USA) with wavenumbers ranging from 400 to 4000 cm^{-1} . Hydrogen bonding interactions were characterized under *in-situ* variable temperature conditions in the temperature range 25-200 °C using infrared spectroscopy employing a Bruker Vertex 80 V Fourier transform infrared spectrometer. Atomic force microscopy (AFM, SPI3800N, Seiko Instruments Inc., Japan) was used to measure the surface morphology of the coating. The particle size and zeta potential values of the system were measured by a Zetasizer Nano ZS (Malvern). Tensile measurements were performed on a CMT6104 universal testing machine (Shenzhen SANS Material Detection Co., Ltd. China) according to ISO 1798: 2008. Compression stress/strain measurements were performed using the Instron 5944 (Instron Corporation, High Wycombe, UK) instrument. The foam samples were cyclically compressed between two metallic plates up to 50% strain at a strain rate of 10%/min. The test was repeated at least 5 times for each formulation in order to ensure reproducibility. The flammability properties of the coated foams were evaluated by horizontal burning test according to ASTM D 4986 standard. And a qualitative visual experiment on the self-extinguishing property of foam burning was performed through a simple horizontal ignition test. The sample

ignition test condition was that the butane igniter was used to ignite the horizontally placed foam sample ($2 \times 2 \times 2 \text{ cm}^3$), the ignition time lasted for 15 s, and the flame length was 2 cm. After removing the fire, we used a camera to take a record to observe the burning process of the foam. All samples were tested under the same conditions, and five samples were repeated, and the sample with the longest burning time was selected to reflect its self-extinguishing performance. Cone calorimeter (CC) tests were performed by a cone calorimeter at a heat flux of 35 kW/m^2 according to ISO 5660-1 standard. The GASMET Fourier transform infrared spectrometer was combined with a cone calorimeter through the heating pipeline to analyze the toxic gases in the combustion flue gas. Raman spectroscopy was carried out at a DXR2xi Raman imaging microscope (Thermo Scientific Co., US). X-ray diffraction (XRD) results were performed on a powder X-ray diffraction (XRD, LabX XRD-6100, Shimadzu, Japan).

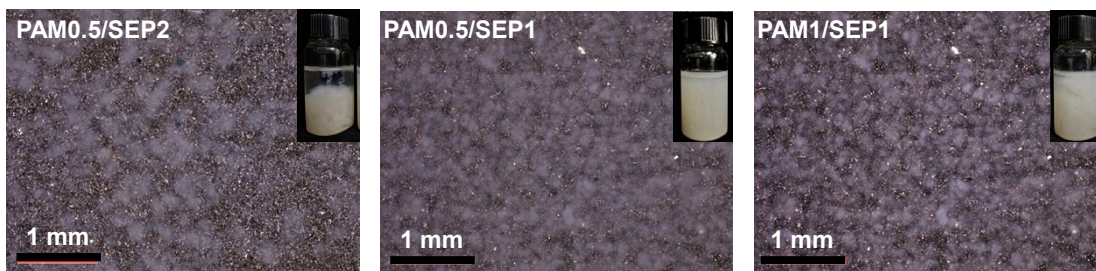


Figure S1. Digital and optical microscope images of PAM/SEP floes assembled by complexation of PAM.

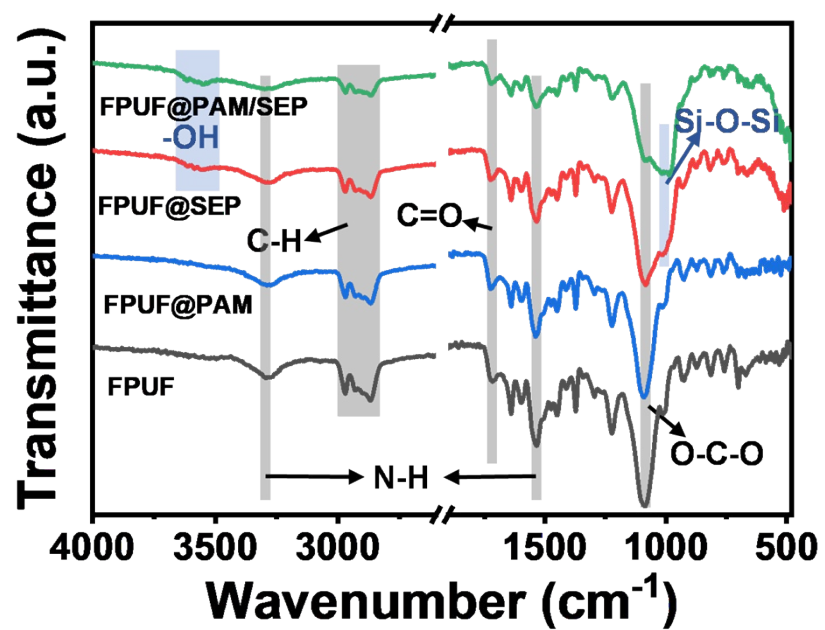


Figure S2. FTIR spectra of neat FPUF, PAM, SEP and PAM/SEP coated foams.

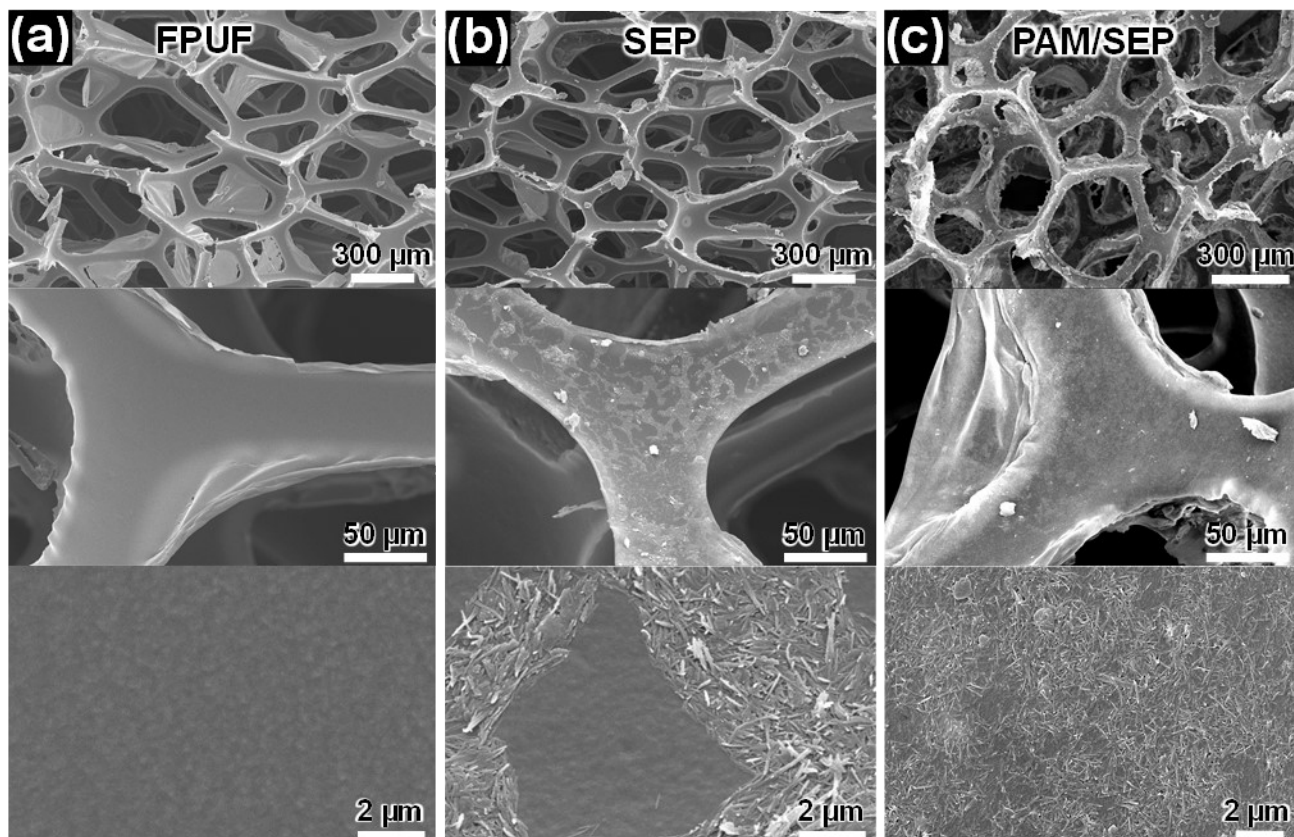


Figure S3. SEM images for the surface morphology of the foams: (a) neat FPUF, (b) dip-coated SEP foam, (c) flocculation-assembled PAM/SEP foam.

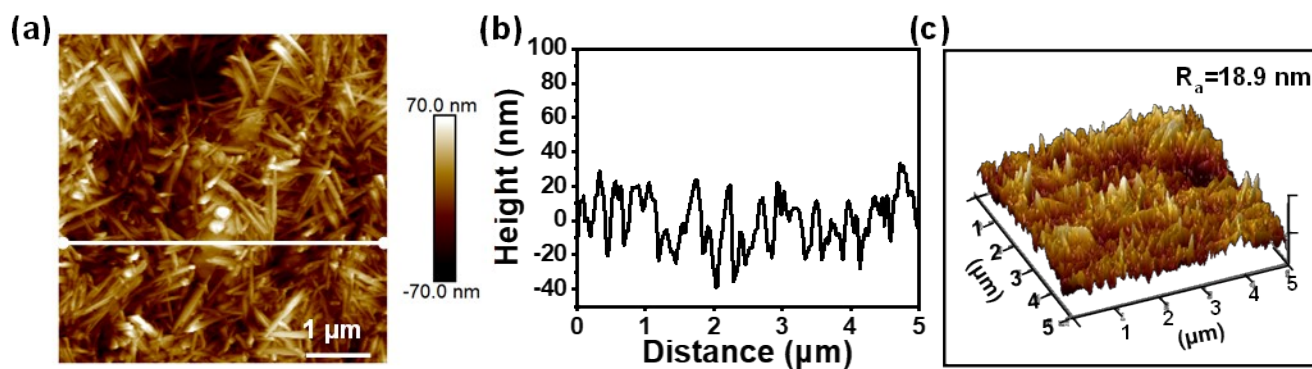


Figure S4. (a) AFM height image of PAM/SEP@Si; (b) height fluctuation along the white line from (a) the AFM height image of PAM/SEP@Si; (c) 3D AFM height image of PAM/SEP@Si.

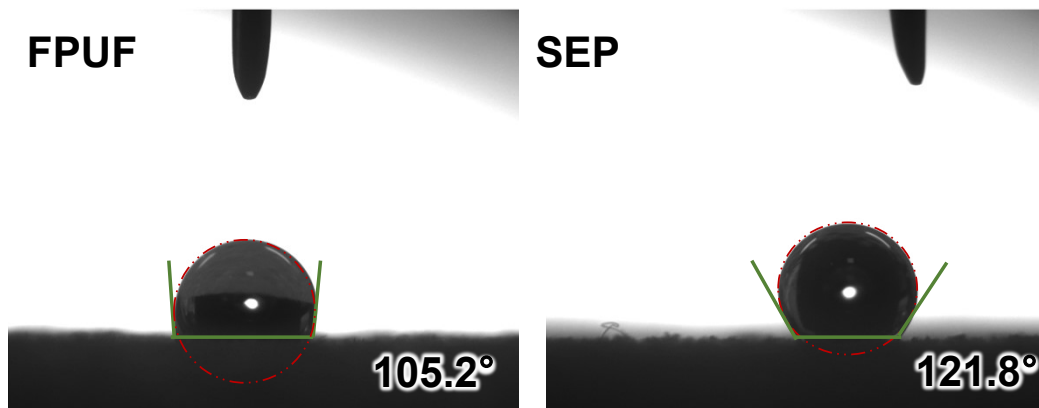


Figure S5. Typical digital images and water contact angle values of neat PU foam and SEP coated foam

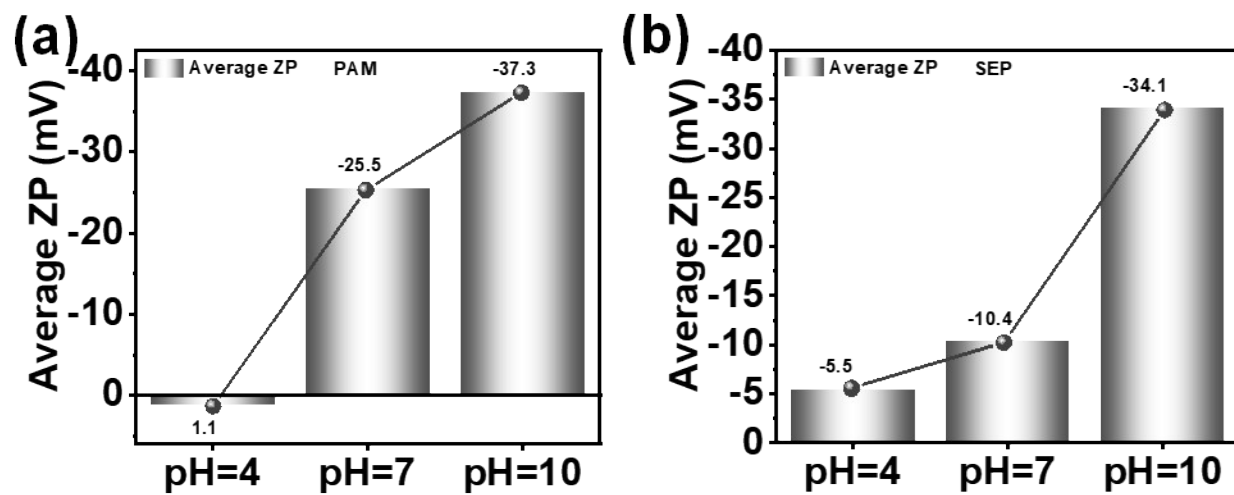


Figure S6. Zeta potential values of PAM (a) and SEP (b) under different pH conditions.

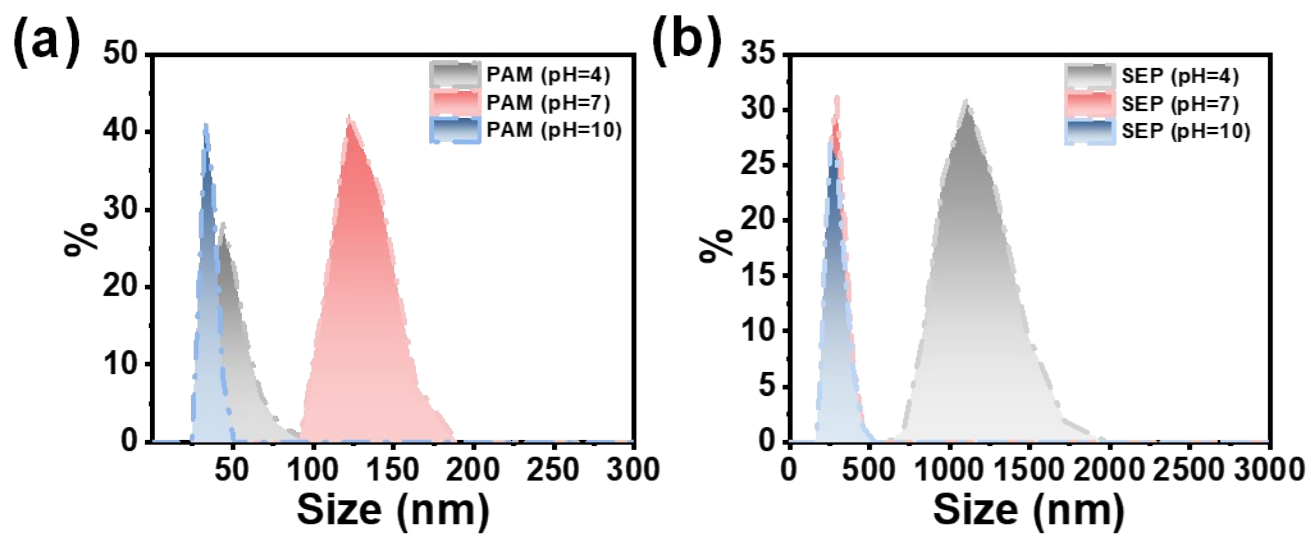


Figure S7. Size distribution of PAM (a) and SEP (b) under different pH conditions.

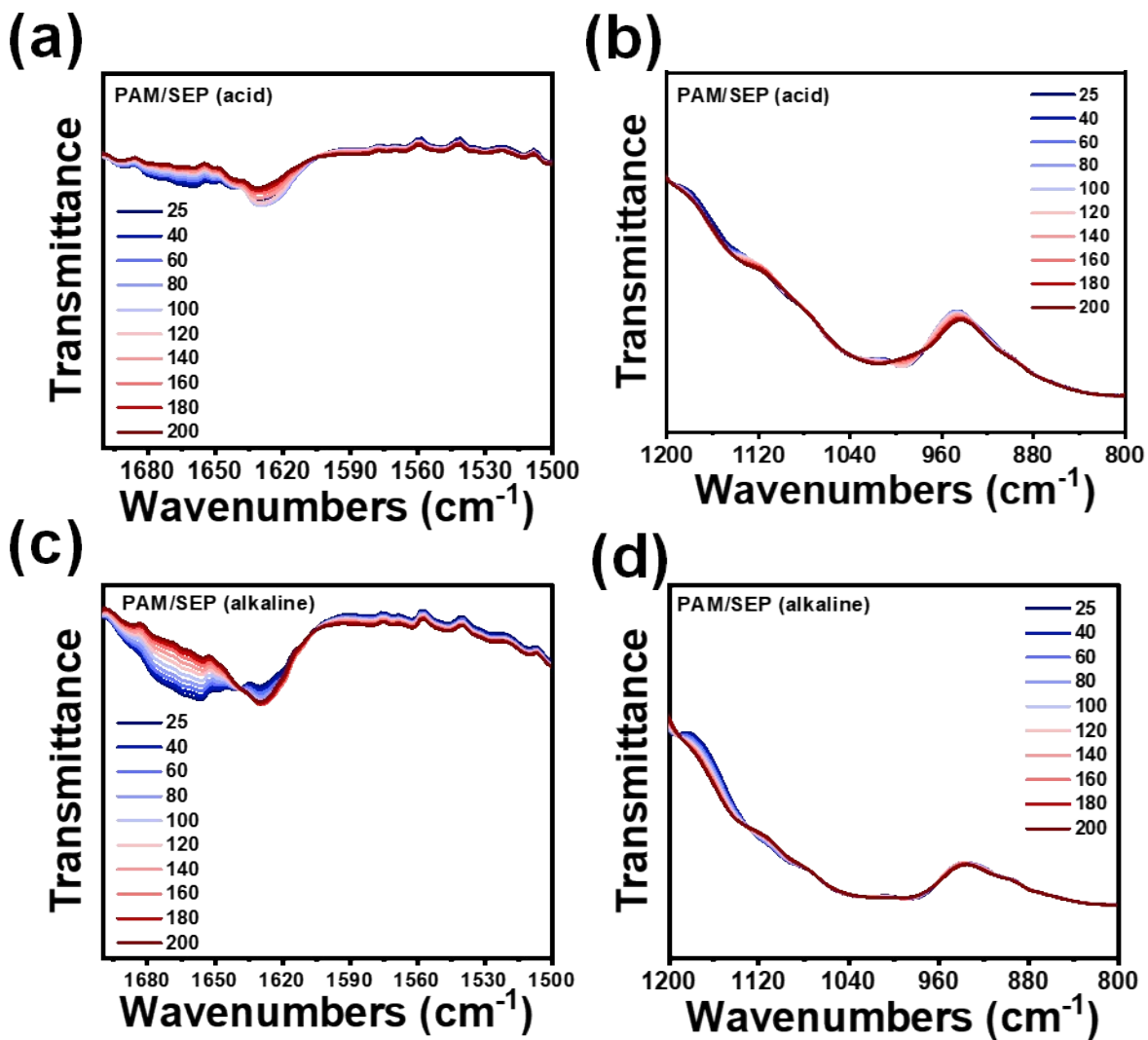


Figure S8. In situ FTIR spectra of the typical peaks of the C-N, Si-O, and C=O groups for PAM/SEP coating under acidic (a,b) and alkaline (c,d) conditions.

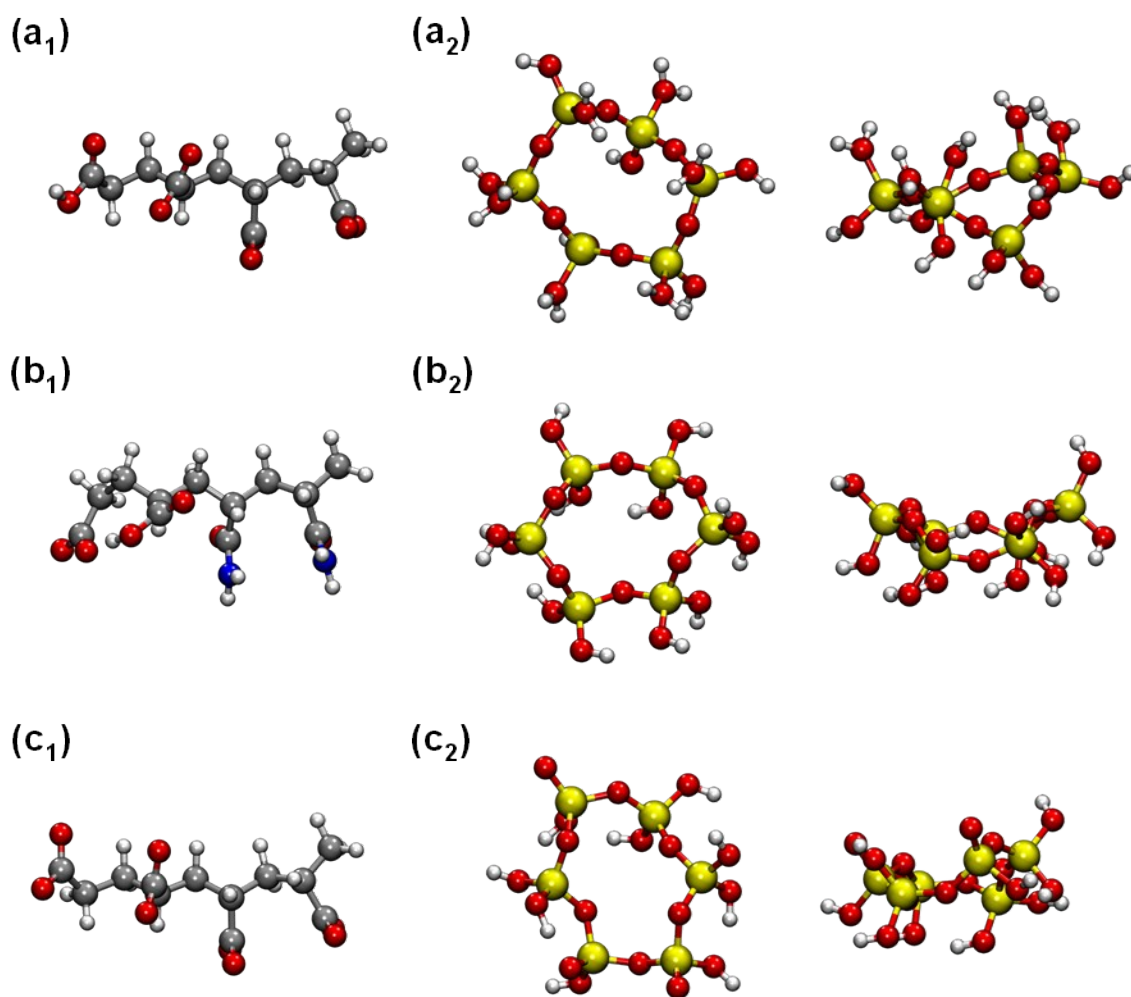


Figure S9. The optimized molecular models of PAM and SEP under acidic (a₁,a₂), neutral (b₁,b₂) and alkaline (c₁,c₂) conditions. Representing colors: hydrogen, white; carbon, black; nitrogen, blue; oxygen, red; silicon, melon yellow.

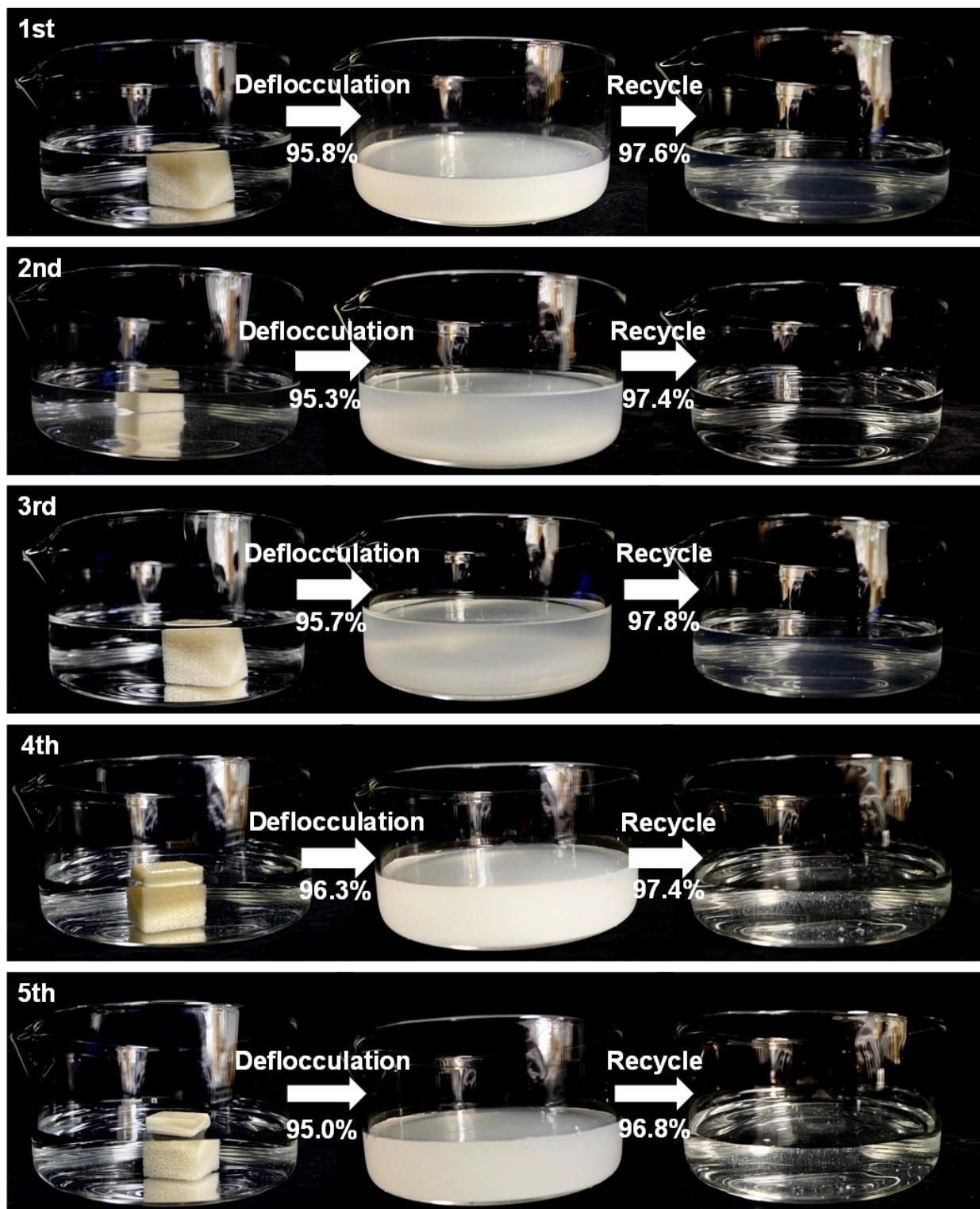


Figure S10. Digital photos of 5 assembly-disassembly cycles of PAM/SEP coated foam.

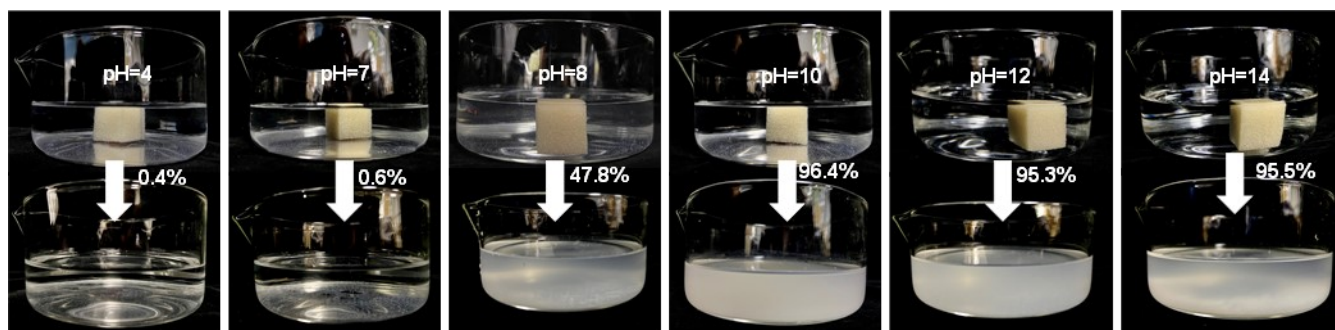


Figure S11. Digital photos of the disassembly processes of PAM/SEP coated foam at different pH values.

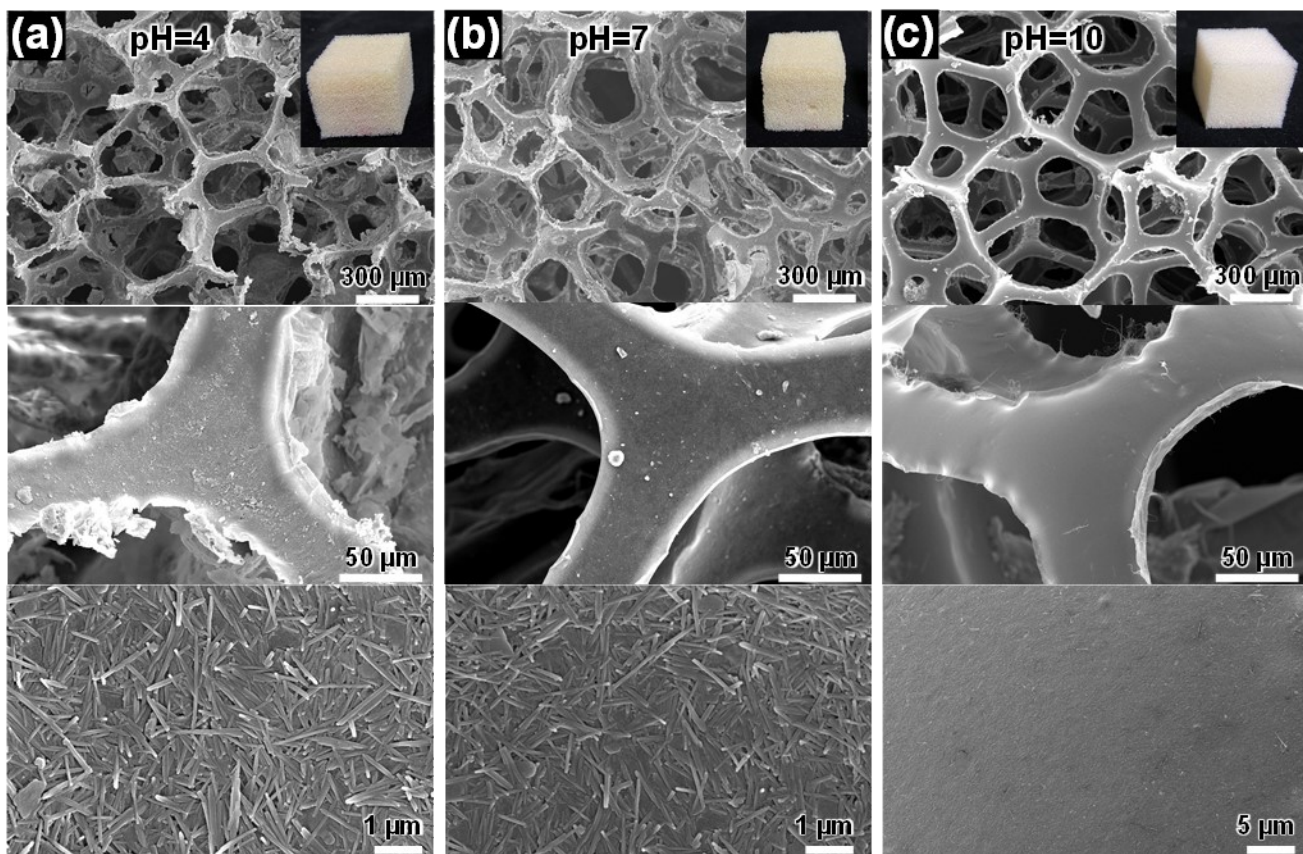


Figure S12. SEM images of the disassembly processes of PAM/SEP coated foam under acidic (a), neutral (b) and alkaline (c) conditions.

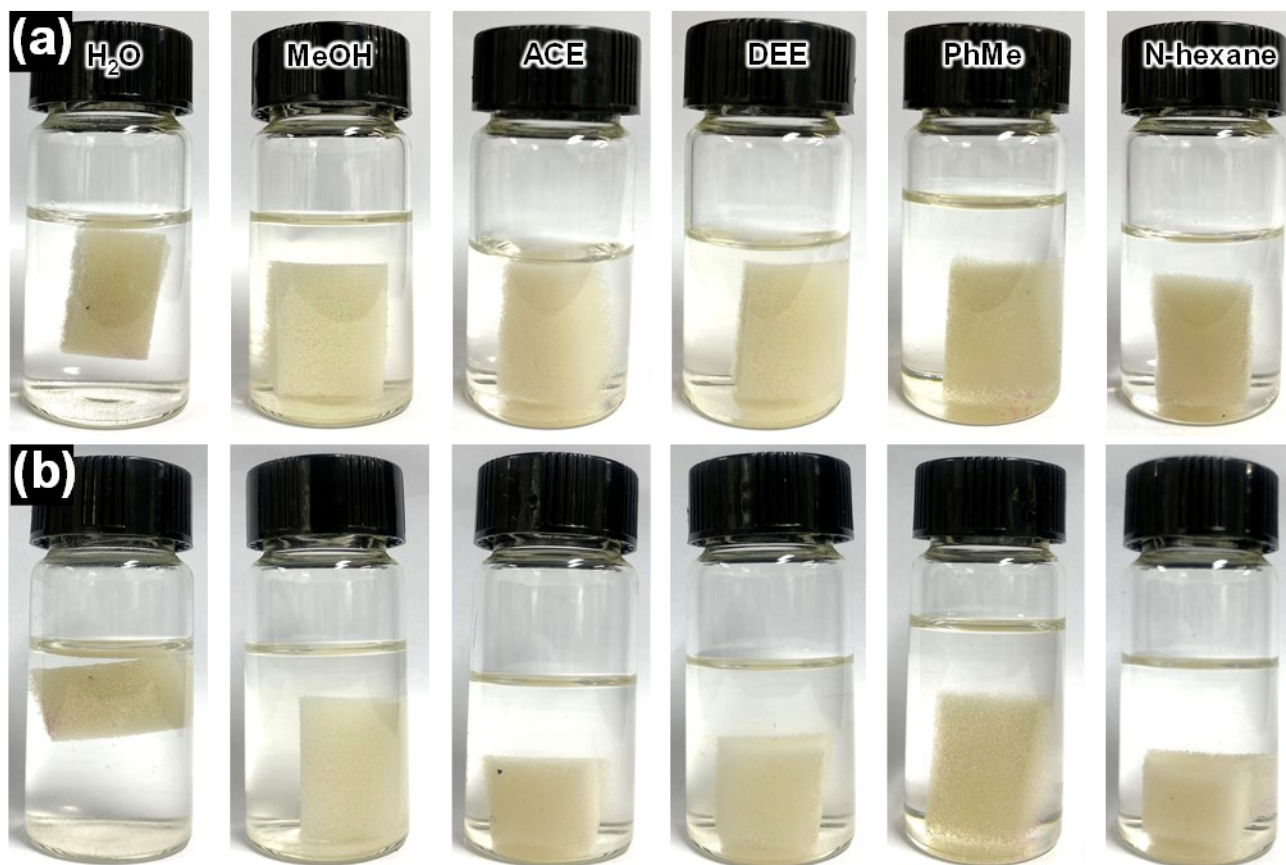


Figure S13. Digital photos of PAM / SEP coated foam soaked in water, methanol, acetone, ether, toluene, hexane and other organic solvents at the beginning (a) and after two weeks (b).

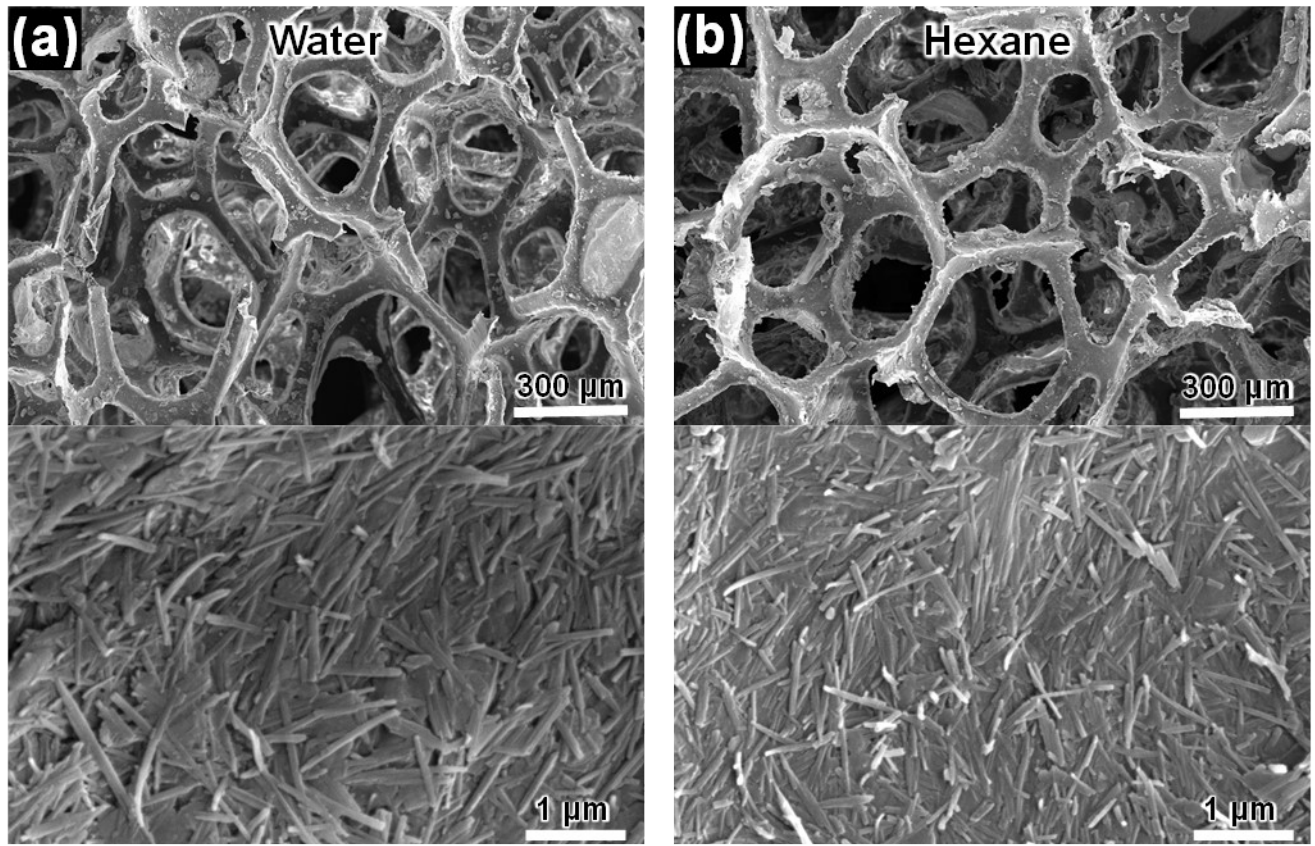


Figure S14. SEM images for surface microstructures of the coated foam after underwater (a) and chemical exposure (b).

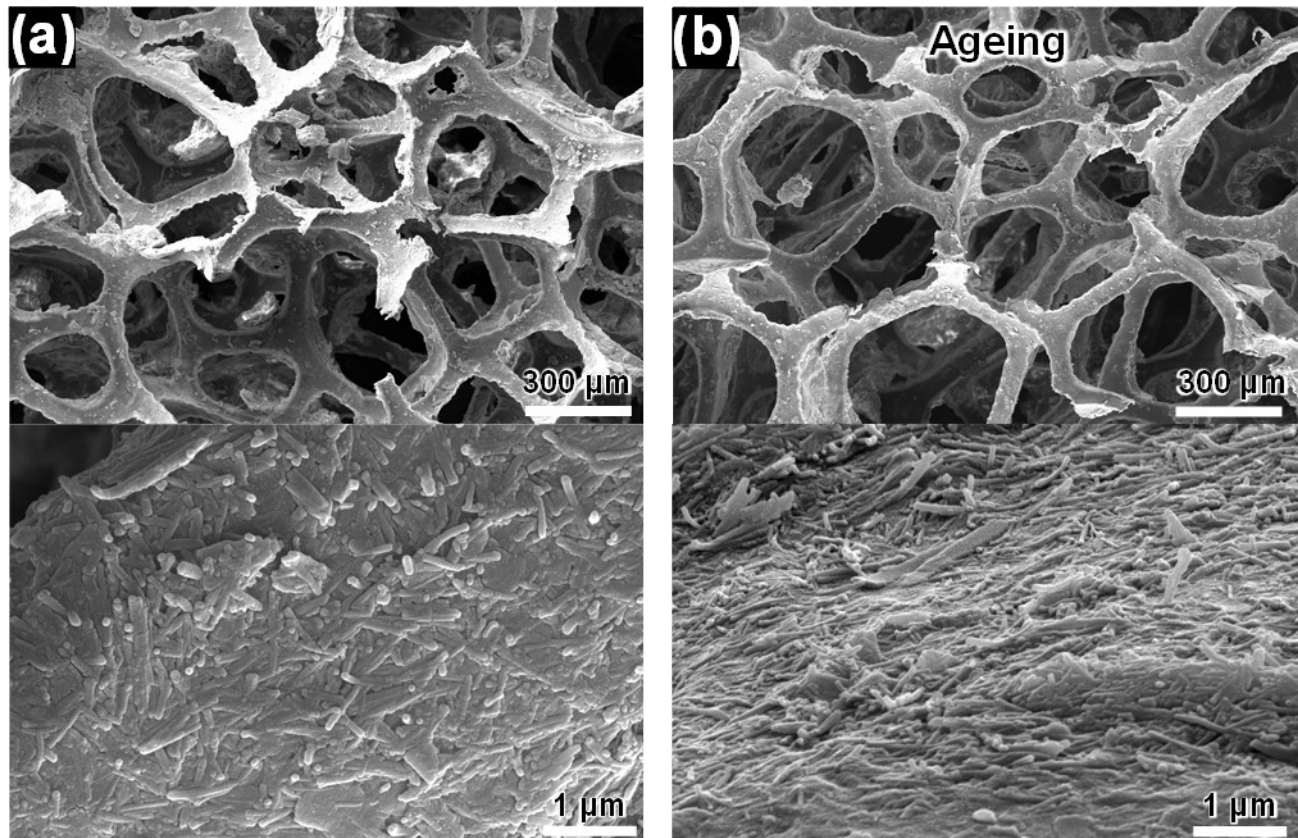


Figure S15. SEM images for surface microstructures of the coated foam after compression treatments before (a) and after aging (b).

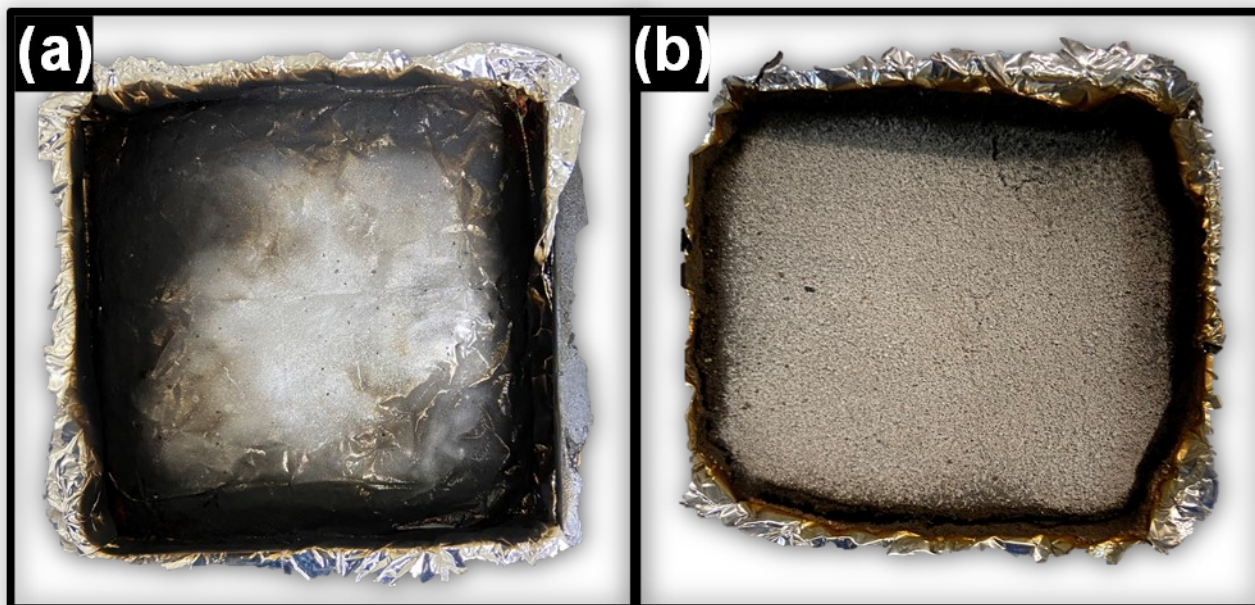


Figure S16. Digital photos of the residue chars for FPUF (a) and PAM/SEP coated foam (b) after cone calorimeter test.

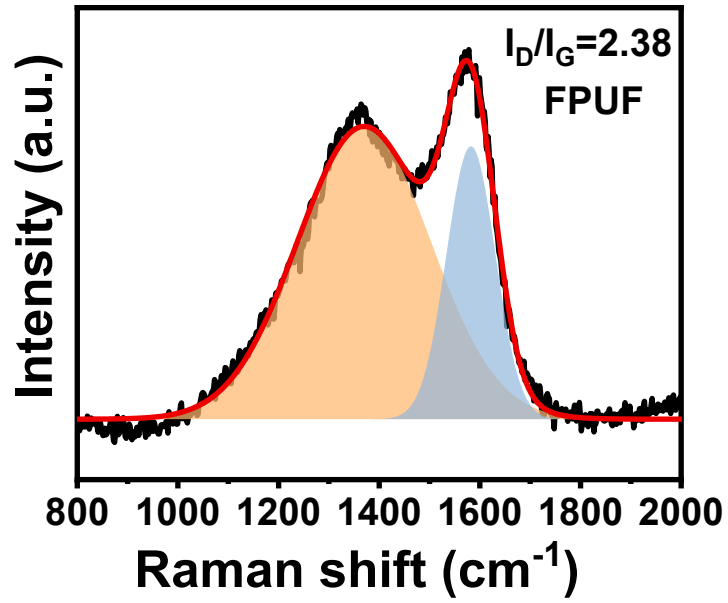


Figure S17. Raman spectra of char residue of FPUF after cone calorimeter test.

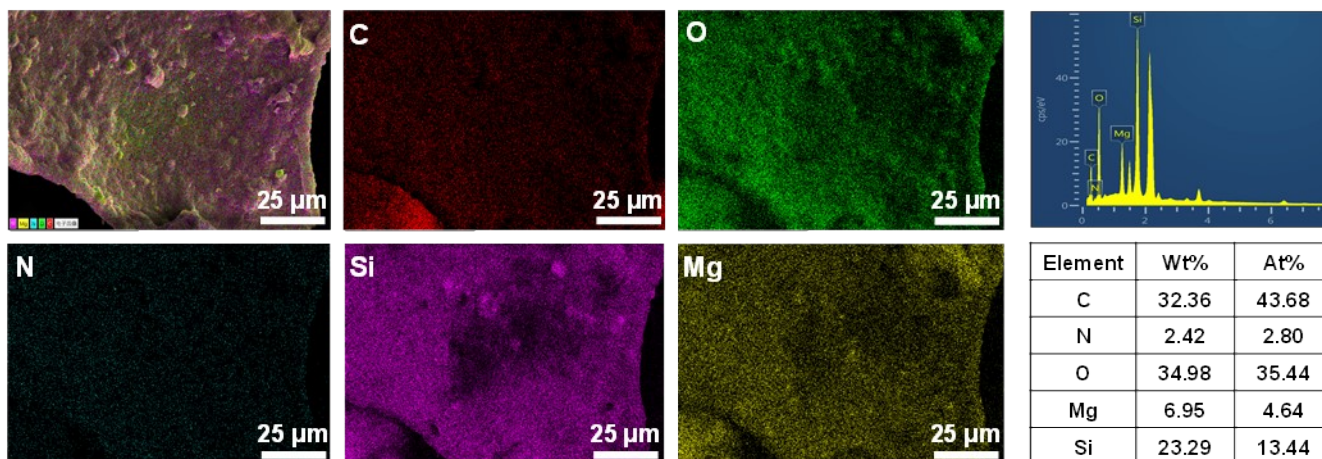


Figure S18. Elemental composition mapping of the char residue for PAM/SEP coated foam after cone calorimeter test.

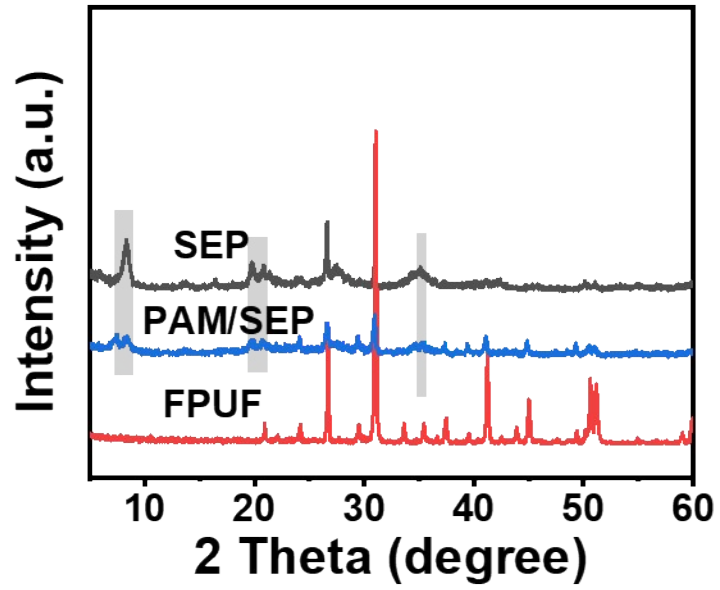


Figure S19. XRD patterns of char residues for FPUF, SEP and PAM/SEP coated foams.

Figure S20. IR spectra of char residues for FPUF, SEP and PAM/SEP coated foams.

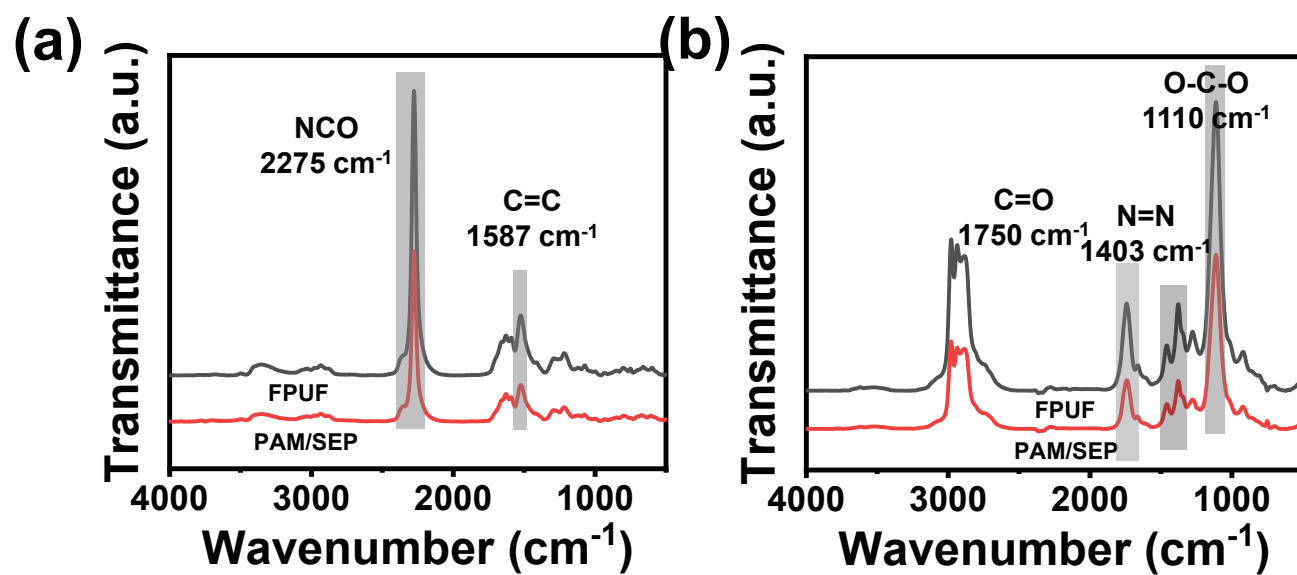


Figure S21. IR spectra of gaseous products of FPUF and PAM/SEP coated foam at the thermal decomposition of the hard (a) and soft segments (b).

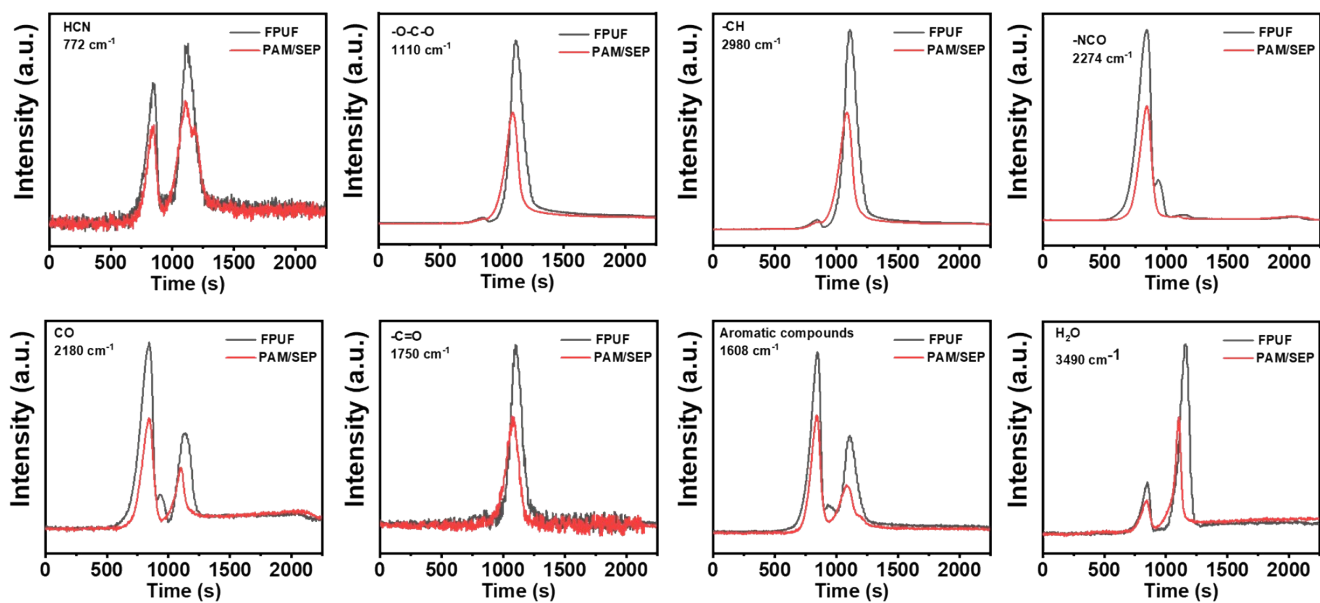


Figure S22. Intensities of characteristic peaks for pyrolysis products of FPUF and PAM/SEP coated foam.

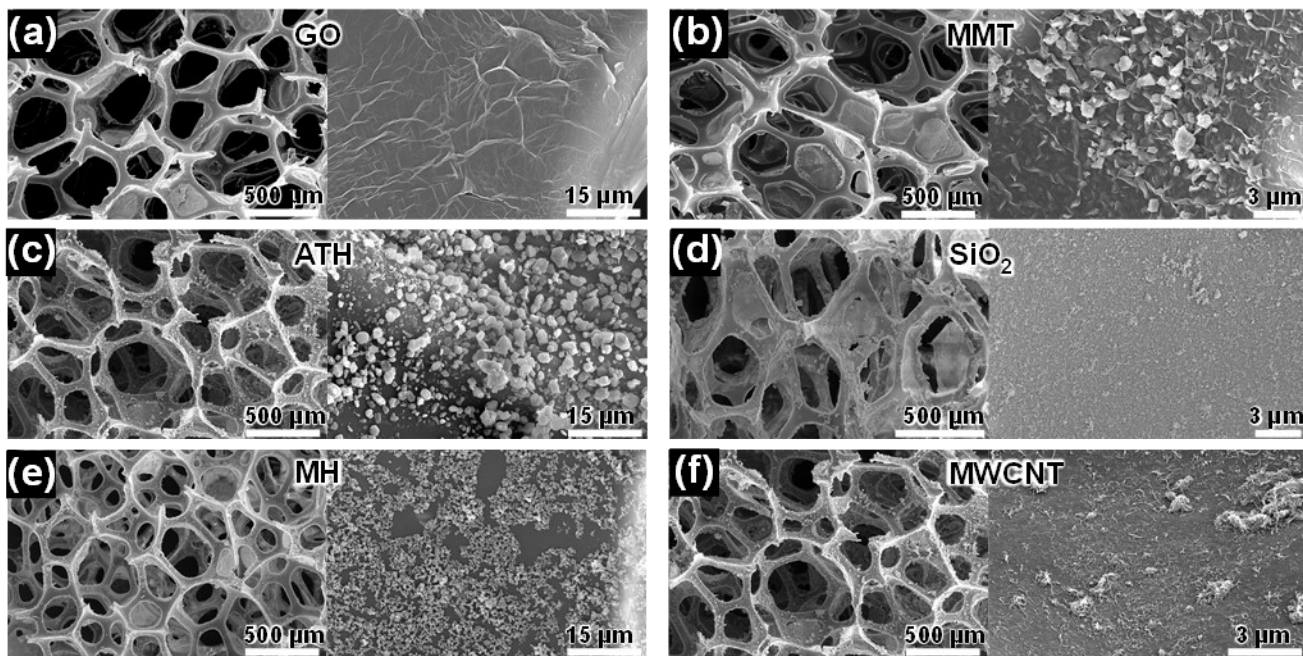


Figure S23. SEM images of lamellar graphene oxide (GO) (a), montmorillonite (MMT) (b), granular aluminum hydroxide (ATH) (c), silica (SiO_2) (d), magnesium hydroxide (MH), (e) and fibrous multiwalled carbon nanotubes (MWCNTs) (f) coated foams by flocculation assembly.

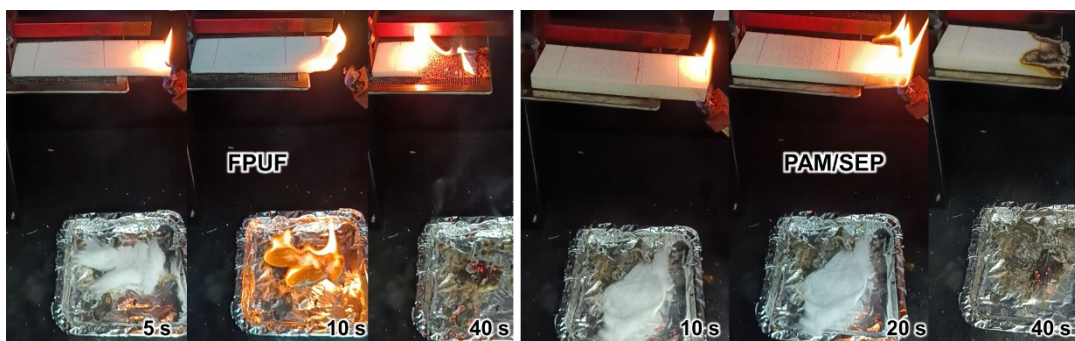


Figure S24 Digital photos of PAM/SEP coated foam in the horizontal burning test.

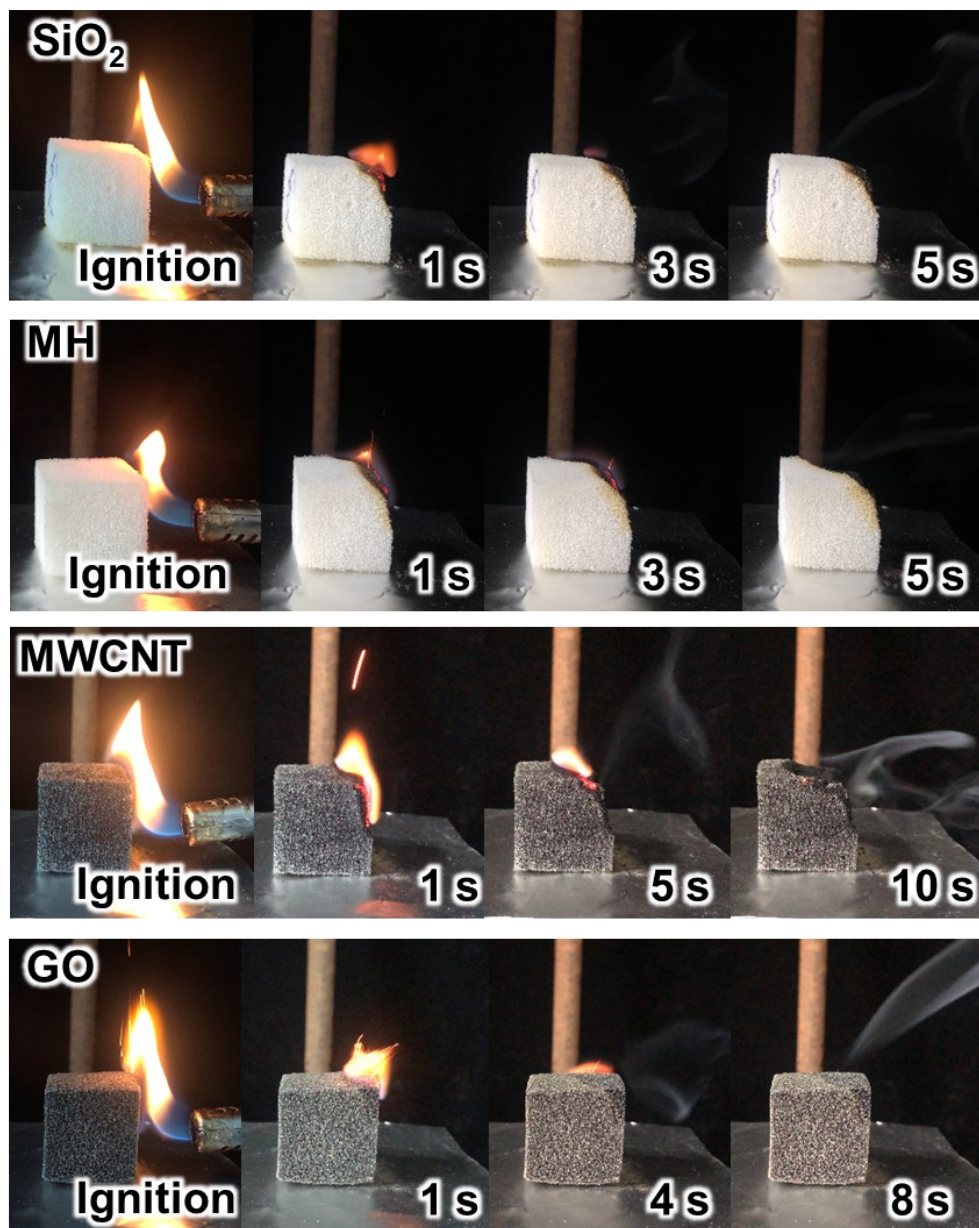


Figure S25. Digital photos of self-extinguishing behavior of various inorganic particle coated foams.

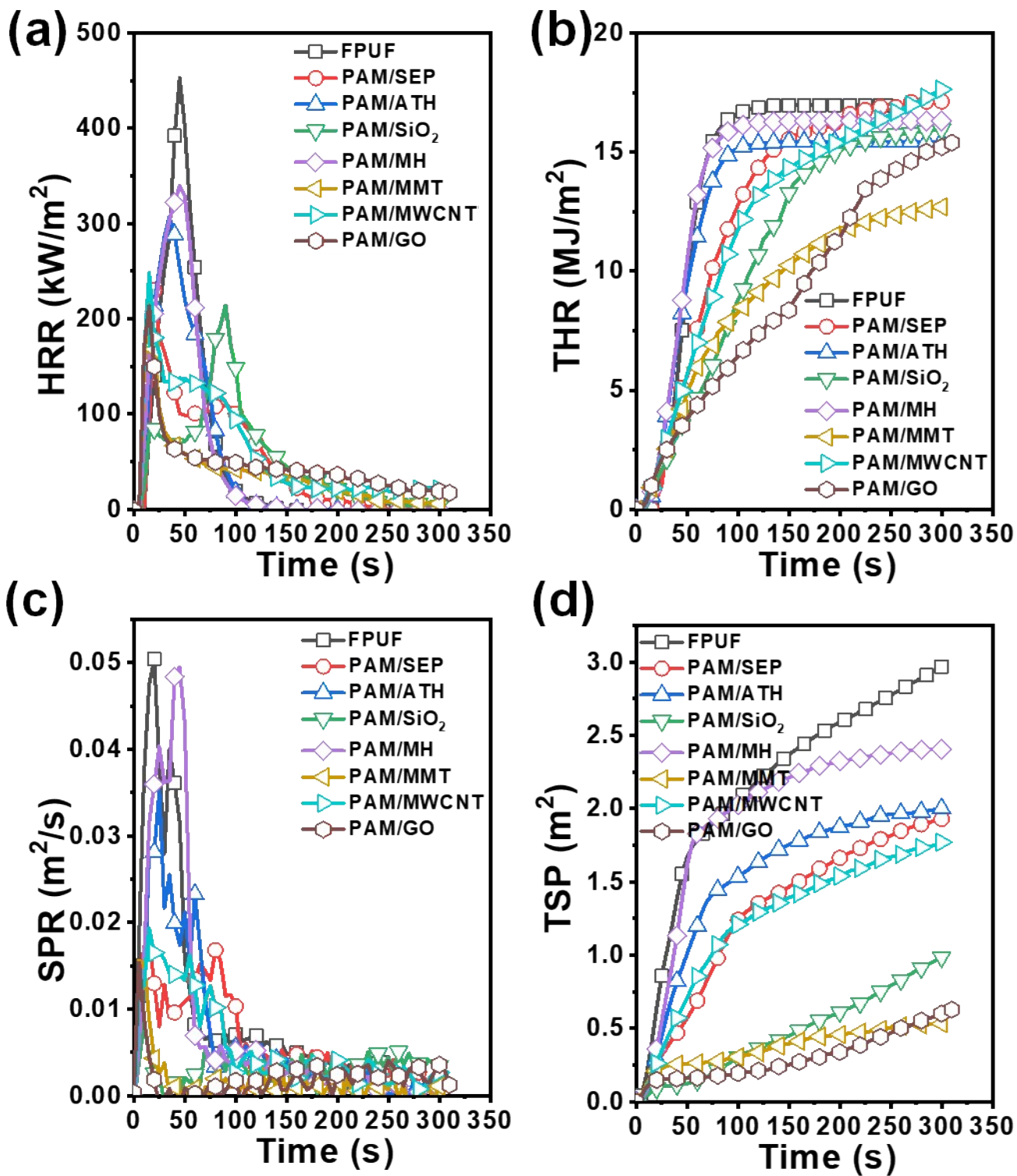


Figure S26. Heat release rate (HRR) (a), total heat release (THR) (b), smoke production rate (SPR) (c) and total smoke production (TSP) (d) curves of the neat FPUF and various inorganic nanoparticles coated foams.

Table S1. The fabrication formulation of the coatings for various samples.

Samples	Water (mL)	PAM (g)	Inorganic particles (g)	Weight gain (wt%)
FPUF	-	-	-	-
FPUF@SEP	100	-	1.0	13.7
FPUF@PAM/SEP^a	100	0.5	1.0	30.8
FPUF@PAM/GO	100	0.5	1.0	18.5
FPUF@PAM/MMT	100	0.5	1.0	31.2
FPUF@PAM/MWCNTs	100	0.5	1.0	27.6
FPUF@PAM/ATH	100	0.5	1.0	33.2
FPUF@PAM/MH	100	0.5	1.0	30.1
FPUF@PAM/SiO₂	100	0.5	1.0	31.3

^a All subsequent studies on PAM/SEP coating are based on this formulation.

Table S2. Binding energy data of the PAM/SEP complex under different pH conditions.

condition	E(a) PAM (kcal/mol)	E(b) SEP (kcal/mol)	E (complex) Complex (kcal/mol)	Eads Binding energy (kcal/mol)
acid	-670,684.249872	-1,946,683.630432	-2617409.021115	-41.1
neutral	-646,319.262099	-1,945,294.375376	-2,591,626.808910	-13.2
base	-1670,393.043189	-1,944,415.87706	-2,614,816.14164	-7.2

$$E_{ads} = E(\text{complex}) - E(a) - E(b)$$

where E_{ads} is the adsorption energy of PAM/SEP complex at different pH states .

where $E(\text{complex})$, $E(a)$ and $E(b)$ are total energies of the complex, PAM and Sepiolite, respectively.

Table S3. Data record of the PAM/SEP coating mass retention rate after immersion in water and various organic solvents for two weeks.

immersion time (days)	Mass retention rate (%)													
	1	2	3	4	5	6	7	8	9	10	11	12	13	14
Water	100	97.8	97.6	97.6	97.5	97.5	97.5	97.4	97.5	97.4	97.3	97.3	97.3	97.3
MeOH	100	99.6	99.4	99.4	99.2	99.1	99.1	99.1	99.0	99.0	99.1	98.9	98.8	98.8
Acetone	100	99.9	99.9	99.8	99.8	99.7	99.6	99.6	99.5	99.5	99.4	99.4	99.4	99.4
Ethyl ether	100	99.9	99.9	99.9	99.8	99.8	99.7	99.7	99.7	99.6	99.6	99.5	99.5	99.5
Toluene	100	100	99.9	99.9	99.9	99.9	99.8	99.8	99.8	99.7	99.6	99.7	99.6	99.6
hexane	100	100	100	99.9	99.9	99.9	99.8	99.8	99.8	99.7	99.8	99.8	99.7	99.8

Table S4. Results of UL-94 horizontal burning test.

Material	Burning time (s)	Distance burned (mm)	Burning drops	Burning rate (mm/min)
FPUF	50	150	Yes	180
PAM/SE P	40	60	Yes	90

Table S5. Cone calorimeter testing data for PU and PAM/SEP coated foams.

Sample	TTI ^a (s)	PHRR ^b (kW/m²)	THR ^c (MJ/m²)	MARHE ^d (kW/m²)	Residue (wt%)
FPUF	1±0	464.0±7.6	17.0±0.6	246.8±5.8	4.0±0.2
PAM/SEP	2±0	222.3±3.2	16.7±0.5	97.8±1.6	21.3±1.4
Ageing	2±0	230.2±3.2	17.0±0.6	99.2±1.7	20.6±1.2
Deflocculation	1±0	435.3±7.5	17.8±0.6	232.5±5.6	5.6±0.2
Recycle	2±0	249.7±3.2	15.5±0.5	102.6±2.0	20.4±1.2

^a The time to ignition; ^b Peak of heat release rate; ^c Total heat release; ^d Maximum average rate of heat emission.

Table S6. Flame retardancy of FPUF coated with multilayered polyelectrolyte+clay coatings in previous reports^a, [1-8]

Coating components	Assembly layers	pHRR	pSPR	Self-extinguishing	Recyclability	Durability	Ref
CH/TiO ₂ /AL	8 TL	-70%	-62%	/	/	/	[1]
PAA/AL/MnO ₂	6 TL	-54%	/	/	/	/	[2]
CH/MXene	8 BL	-57%	-60%	/	/	/	[3]
PEI/ β -FeOOH/AL	8 TL	-62%	-35%	/	/	/	[4]
CS/VMT-CS/APP	24 BL	-66%	/	Yes	/	/	[5]
CS/AL/GO	10 TL	-60%	-46%	Yes	/	/	[6]
CS/MMT	10 BL	-52%	/	Yes	/	/	[7]
CH/MoS ₂	8 BL	-70%	-62%	Yes	/	/	[8]
PAM/SEP	/	-52%	-72%	Yes	Yes	Yes	This work

^a All coated samples were carried out according to ISO 5660 standard under 35 kW/m² heat radiation flux and 25 mm sample thickness.

- [1] H. F. Pan, W. Wang, Y. Pan, L. Song, Y. Hu, K. M. Liew, *ACS Appl. Mater. Interfaces*, 2015, **7**, 101–111.
- [2] W. Wang, Y. Pan, H. Pan, W. Yang, K. M. Liew, L. Song, Y. Hu, *Compos. Sci. Technol.*, 2016, **123**, 212–221.
- [3] B. Lin, A. C. Y. Yuen, A. Li, Y. Zhang, T. B. Y. Chen, B. Yu, E. W. M. Lee, S. Peng, W. Yang, H. D. Lu, Q. N. Chan, G. H. Yeoh, C. H. Wang, *J. Hazard. Mater.*, 2020, **381**, 120952.
- [4] H. F. Pan, Y. Pan, L. Song, Y. Hu, *Polym. Adv. Technol.*, 2017, **28**, 243–251.
- [5] K. M. Holder, M. E. Huff, M. N. Cosio, J. C. Grunlan, *J. Mater. Sci.*, 2015, **50**, 2451–2458.
- [6] X. Zhang, Q. Shen, X. Zhang, H. Pan, Y. Lu, *J Mater Sci.*, 2016, **51**, 0361–0374.
- [7] G. Laufer, C. Kirkland, A. A. Cain, J. C. Grunlan, *ACS Appl. Mater. Interfaces*, 2012, **4**, 1643–1649.
- [8] H. F. Pan, Q. Shen, Z. N. Zhang, B. H. Yu, Y. S. Lu, *J Mater Sci.*, 2018, **53**, 9340–9349.

Table S7. Cone calorimeter testing data for PU and various inorganic particles coated foams.

Sample	TTI^a (s)	PHRR^b (kW/m²)	THR^c (MJ/m²)	MARHE^d (kW/m²)	PSPR^e (m²/s)	TSP^f (m²)	Residue (wt%)
FPUF	1±0	464.0±7.6	17.0±0.6	246.8±5.8	0.0609±0.0042	2.97±0.08	4.0±0.2
PAM/SEP	3±1	222.3±5.5	16.7±0.5	97.8±1.6	0.0172±0.0014	1.93±0.06	39.6±1.6
PAM/ATH	3±1	307.7±5.9	17.2±0.6	190.6±2.7	0.0352±0.0025	2.00±0.07	37.4±1.5
PAM/SiO₂	4±1	214.1±4.5	16.0±0.5	80.7±1.2	0.0084±0.0007	0.99±0.02	52.1±3.2
PAM/MH	3±1	339.7±6.1	17.8±0.6	220.1±3.6	0.0495±0.0032	2.41±0.07	27.2±1.0
PAM/MMT	3±1	232.4±3.4	12.7±0.4	84.8±1.3	0.0155±0.0011	0.53±0.01	38.2±1.6
PAM/MWCNT	3±1	248.8±3.7	17.6±0.6	119.2±1.8	0.0193±0.0015	1.77±0.05	29.1±1.3
PAM/GO	2±0	213.3±2.9	15.4±0.5	83.7±1.4	0.0153±0.0010	0.63±0.01	21.0±0.9

^a The time to ignition; ^b Peak of heat release rate; ^c Total heat release; ^d Maximum average rate of heat emission; ^e Peak of smoke production rate; ^f Total smoke production.